

Singlet oxygen production analysis of reduced berberine analogs via NMR spectroscopy

Sarah Su^{1,2}, Emma Le^{3,2}, Pratyush Singh^{4,2}, Karthikha Sri Indran^{5,2}, Sohie Pal^{6,2}, Anika Regan^{7,2}, Meher Jain^{5,2}, Aashi Shah^{3,2}, Edward Njoo²

¹Los Altos High School, Los Altos, CA

²Department of Chemistry, Biochemistry, & Physical Science, Aspiring Scholars Directed Research Program, Fremont, CA

³Amador Valley High School, Pleasanton, CA

⁴American High School, Fremont, CA

⁵Mission San Jose High School, Fremont, CA

⁶Carlmont High School, Belmont, CA

⁷BASIS Independent Silicon Valley, San Jose, CA

SUMMARY

Berberine is a natural product isoquinoline alkaloid derived from plants of the genus *Berberis*. When exposed to photoirradiation, it produces singlet oxygen through photosensitization of triplet oxygen. The production of singlet oxygen grants Berberine its biological activity, as singlet oxygen forms an activated complex with DNA, oxidizing its guanine residues, halting cell replication and leading to cell death, which can be applied in photodynamic therapy of cancer. Through qNMR analysis of ¹H NMR spectra gathered through kinetic experiments, we were able to track the generation of a product between singlet oxygen and alpha terpinene, allowing us to quantitatively measure the photosensitizing properties of our scaffolds. Moreover, we implemented 7,8-dihydroberberine and tetrahydroberberine, the reduced and over-reduced forms of berberine, respectively, in the studies to test the effect of the reduction of a compound on its singlet oxygen production.

INTRODUCTION

Singlet oxygen production is harnessed by nature as a means of introducing reactive oxygen species into chemical systems in a variety of contexts, including biosynthesis, ecological remediation, and therapeutics. Singlet oxygen is a reactive oxygen species known to participate in 4+2 cycloadditions with 1,3 diene systems as well as ene reactions with electron-rich alkenes (1-4). Production of singlet oxygen is mediated by photosensitizing agents, which undergo initial photoexcitation, followed by intersystem crossing and phosphorescence to excite diatomic oxygen from the ground triplet state to an excited singlet state (5).

More specifically, singlet oxygen has been used in nature to perform highly selective oxidations in key biosynthetic routes, and this has been emulated in biomimetic synthetic approaches to natural products (6). Moreover, reactive oxygen species have the ability to induce cell death via oxidative damage of key biomolecules, including DNA (7). Singlet oxygen is especially reactive compared to triplet

oxygen, as it has paired electrons in its π antibonding 2p orbital (8). As such, *in situ* generation of singlet oxygen has the potential to be used in various medicinal settings, such as in the photodynamic therapy of cancer (9).

While singlet oxygen generation can be modulated efficiently with various commercially available photosensitizers, naturally-derived, chromogenic small molecules are also available for singlet oxygen production (10). One such molecule, berberine, is a DNA-binding natural product alkaloid isolated from plants of the genus *Berberis* (11). Berberine derives its singlet oxygen photosensitizing properties from its extended polyaromatic scaffold, in which delocalized π electrons are excitable in the near-ultraviolet (UV) range ($\lambda_{max} = 349$ nm) (12). As berberine binds to DNA, the generation of reactive oxygen species leads to specific oxidation of guanine bases, ultimately resulting in cell death (12, 13). Previous studies have shown berberine to be a potent bioactive agent with a diverse array of medicinal properties, including antimicrobial, antidiabetic, and anticancer properties (14, 15).

Previously, we reported a comparison of berberine and two other commercially available compounds in which we found that berberine is a more efficient singlet oxygen photosensitizer than methylene blue but less efficient than rose bengal (16). In addition to berberine, there are two berberine analogs that differ in C-ring oxidation patterns: 7,8-dihydroberberine and tetrahydroberberine. We have previously reported the differences in the photochemically activated antimicrobial activity of berberine and its reduced analog, dihydroberberine (**Figure 1**) (17). However, a thorough investigation of the singlet oxygen production capabilities of these compounds has not been performed. We hypothesized that the berberine analogs 7,8-dihydroberberine and tetrahydroberberine possess sequentially decreased photosensitizing abilities compared to berberine due to the loss of conjugation on the chromophore scaffold of berberine. Thus, through quantifying singlet oxygen production as a function of reduction, we develop a structure-activity relationship between the berberine chemical structure and its photosensitizing

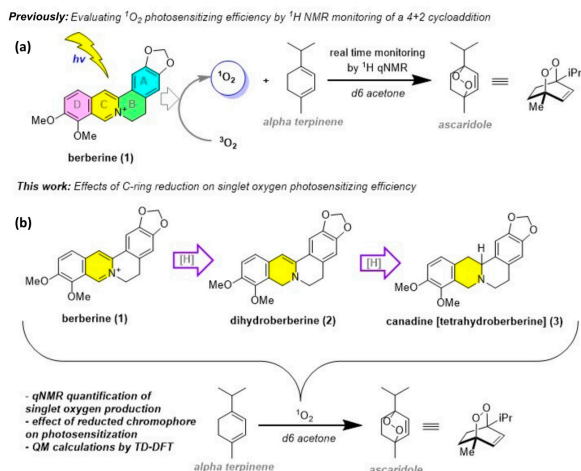


Figure 1: Overview of Study Design in Comparison to Past Work (a) Study design to elucidate the effect of C-ring reduction on singlet oxygen photosensitizing efficiency, as compared to our earlier work on berberine's photosensitizing efficacy in relation to commercially available photosensitizers (16). Both studies employed the use of qNMR and benchtop ^1H NMR to monitor the production of singlet oxygen over time. (b). Berberine and its reduced analogs, 7,8-dihydroberberine and tetrahydroberberine, were assayed in their singlet oxygen photosensitizing properties.

properties in order to direct future synthesis. In this study, we used a similar study design as reported earlier to evaluate the efficacy of berberine in comparison to reduced berberine analogs, 7,8-dihydroberberine, and tetrahydroberberine, in generating singlet oxygen (16) (**Figure 2**).

Through the use of ^1H benchtop nuclear magnetic resonance spectroscopy, we were able to track a 4+2 cycloaddition between singlet oxygen and alpha-terpinene towards quantifying the singlet oxygen production over time in the presence of photosensitizers such as berberine, 7,8-dihydroberberine, and tetrahydroberberine. Moreover,

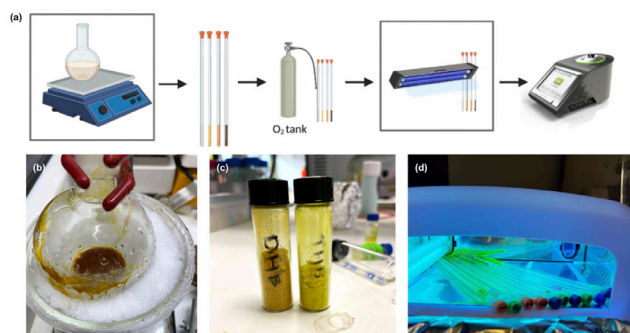


Figure 2: Experimental design and synthesis for photosensitizers in this study. (a) Synthesis and photoirradiation of NMR tubes experiment process. NMR tubes were flushed with oxygen and then irradiated for 60-minute intervals while monitored with ^1H NMR. Endoperoxide formation in alpha-terpinene was allowed, and the data was used to derive the singlet oxygen photosensitizers' efficiency. (b) Recrystallization of reduced berberine analog. (c) Produced yield of 7,8-dihydroberberine (left) and tetrahydroberberine (right). (d) Irradiation of NMR tubes under UV light.

	Berberine	7,8-dihydroberberine	Tetrahydroberberine		Berberine	7,8-dihydroberberine	Tetrahydroberberine
LUMO (+1 (singlet))	eV = -2.11	eV = -0.272	eV = -0.280	LUMO (+1 (triplet))	eV = -2.11	eV = -0.412	eV = -0.333
LUMO (singlet)	eV = -2.777	eV = -1.025	eV = -0.372	LUMO (triplet)	eV = -2.777	eV = -2.342	eV = -1.967
HOMO (singlet)	eV = -5.931	eV = -4.632	eV = -5.572	HOMO (triplet)	eV = -5.931	eV = -5.283	eV = -5.876

Table 1: The excited state molecular orbitals of our tested photosensitizers were modeled with Avogadro after being optimized via ORCA TD-DFT. Orbitals shaded red show regions of positive overlap, and orbitals shaded blue show regions of negative overlap.

we corroborated our results using time-dependent density functional theory (TD-DFT) to observe the HOMO-LUMO gap of our analogs respectively. The use of benchtop NMR spectroscopy to develop a structure-activity relationship of photosensitizers is unprecedented. Through this experiment, we ascertained that reduction had a significant impact on the photosensitizing property of berberine and berberine related scaffolds, where increased reduction decreased the photosensitizing ability of the analogs. We believe that this can direct future synthesis of berberine analogs, as reduction of the chromophore seems to have an averse effect to the biological activity of the compound.

RESULTS

To quantify singlet oxygen production, we utilized alpha-terpinene, a commercially available monoterpene with a cyclic 1,3-diene functionality, to trap singlet oxygen species in a Diels-Alder-like hetero 4+2 cycloaddition, whereby the resulting endoperoxide product was quantified by quantitative nuclear magnetic resonance (qNMR) spectroscopy (18). Using this method, we assayed two reduced berberine analogs against berberine: 7,8-dihydroberberine and tetrahydroberberine (**Figure 1b**).

Computational Modeling of Photosensitizing Capabilities through TD-DFT

All photosensitizers were predicted to be able to generate singlet oxygen based on HOMO-LUMO molecular orbital energy gaps, as all had greater than 0.98 eV of energy from the gap between triplet excited and singlet ground state, as necessary to generate singlet oxygen (**Table 1**) (19). We determined this gap through subtracting the energies of the triplet LUMO and the singlet HOMO. While calculations of the lifetimes of excited states and the kinetics of excited state decay of these compounds were beyond the scope of our current research, Fermi's Golden Rule can be applied to our data to find these characteristics (20).

Interestingly, our TD-DFT calculation results yielded greater HOMO-LUMO energy gaps for the reduced analogs when compared to berberine, suggesting greater photosensitizing efficacy: the energy gap for berberine

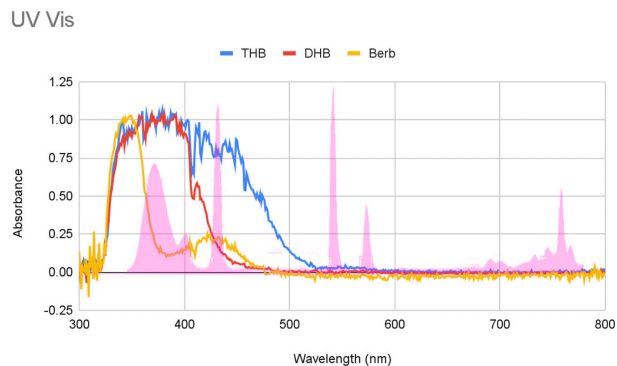


Figure 3: Ultraviolet-visible spectroscopy of berberine (Berb), 7,8-dihydroberberine (DHB), and tetrahydroberberine (THB). Due to the difference in absorbance of our analogs, varying light sources were needed to ensure that all of the samples experienced irradiation within the excitation range of tested photosensitizers.

was 1.932, while the energy gap for dihydroberberine and tetrahydroberberine were 2.290 and 3.605 respectively (Table 1). We sought to corroborate these results with qNMR analysis by tracking the singlet oxygen production efficacy of reduced berberine analogs in comparison to berberine over time.

Synthesis of Berberine Scaffolds and ¹H qNMR analysis of Singlet Oxygen Production

We synthesized 7,8-dihydroberberine (Compound 2) and tetrahydroberberine (Compound 3) from commercially available berberine chloride (Figure 1b). Dihydroberberine and tetrahydroberberine were both prepared through a borohydride-mediated reduction of berberine, wherein adjusting the reaction time can selectively produce 7,8-dihydroberberine or the fully-reduced tetrahydroberberine (Figure 1b) (21). All three berberine analogs were irradiated

with UV light with the following UV emission spectrum ranging from 350 to 800 nm (Figure 3) in 60-minute periods, with NMR spectra taken during the intervals.

We used qNMR analysis to derive a quantification of singlet oxygen production as a function of time. To do so, we used alpha terpinene to serve as a substrate which would react with singlet oxygen to form ascaridole and cymene, which we could track via ¹H NMR. We tested our photosensitizers through observing the formation of ascaridole and cymene in the presence of various photosensitizers against a control trial, which did not have a photosensitizer.

Ascaridole and cymene, which were the products of the 4+2 cycloaddition between singlet oxygen and alpha terpinene, were revealed through the appearance of peaks with a chemical shift of 6.44 ppm and 7.13 ppm, respectively, and were used to calculate the concentrations of products through qNMR (Figure 4). Endoperoxide and p-cymene concentrations were measured over time and the sum of their integrations was used to determine total effective singlet oxygen production, which was graphed as shown below (Figure 5).

We found that for hours 0 and 1, berberine, 7,8-dihydroberberine, and tetrahydroberberine performed similarly, and for time period 0, their singlet oxygen production was not significantly different from the control. However, for time periods 2 through 5, the reduced analogs had significantly lower singlet oxygen photosensitizing efficacy relative to berberine (Figure 5).

DISCUSSION

Owing to the centrality of in vivo singlet oxygen production in driving berberine's biological activity, measuring singlet oxygen production effectively offers insight into berberine's medicinal efficacy. Moreover, evaluation of the singlet oxygen

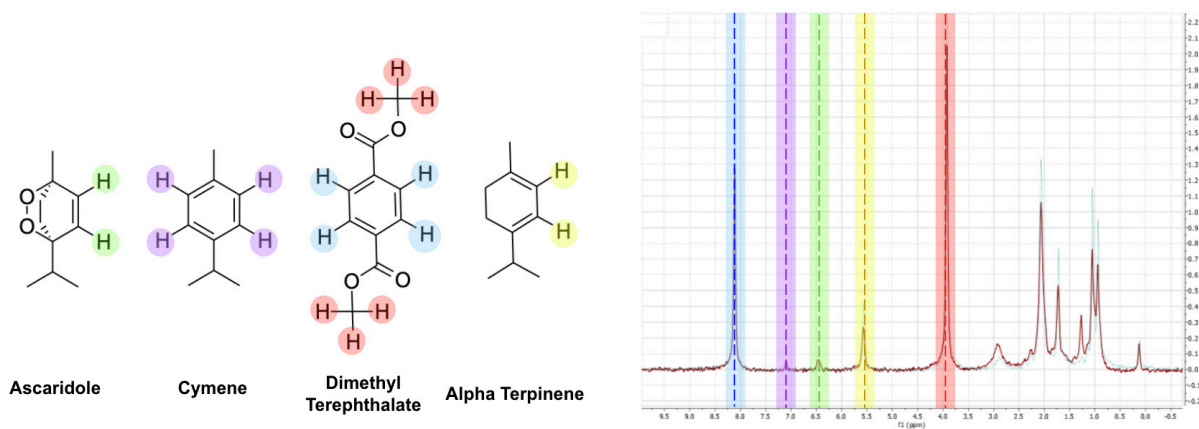


Figure 4: The vinyl protons of the endoperoxide on ascaridole were characterized through a doublet at 6.44 ppm. P-cymene, a minor oxidative product, was characterized through aromatic protons corresponding to a doublet of doublets at 7.13 ppm. Alpha terpinene was revealed through its vinyl protons with a doublet at 5.5 ppm, and the internal standard, dimethyl terephthalate, was characterized through a doublet of doublets at ~8.1 ppm and a singlet at ~4.0 ppm.

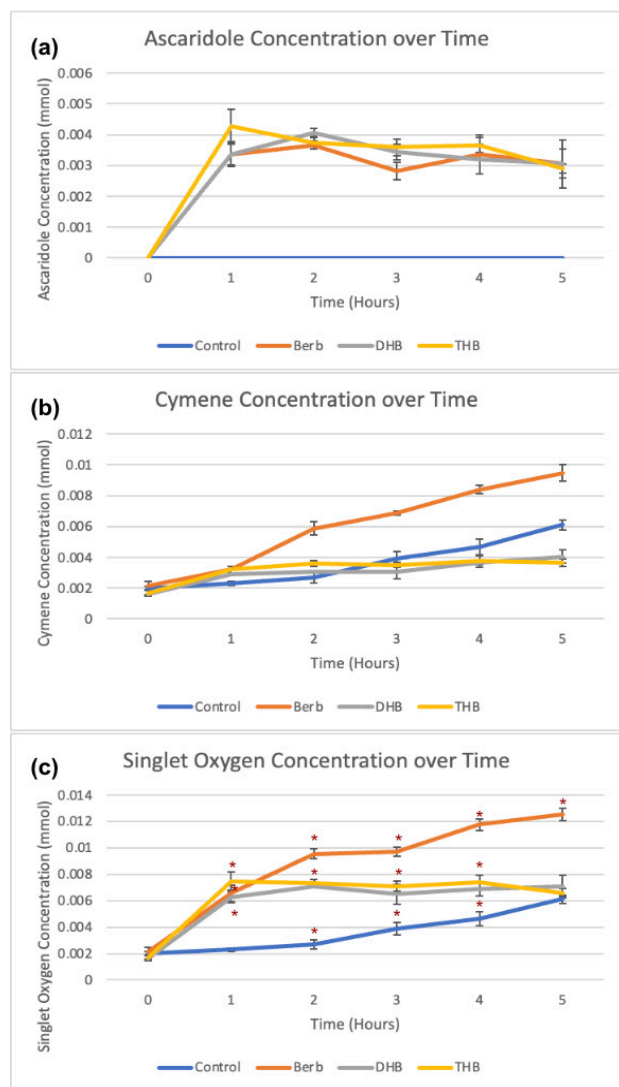


Figure 5. Ascaridole, cymene, and singlet oxygen formation rates found through ^1H NMR kinetics experiments. Results for controls are noted in blue, berberine in orange, dihydroberberine in gray, and tetrahydroberberine in yellow. Data was taken in triplicate, with error bars representing the standard deviation between trials. Production of ascaridole and cymene, the products of the 4+2 cycloaddition between singlet oxygen and alpha terpinene, were graphed against time in parts (a) and (b) respectively. The cymene formation shown in the control group in part (b) is likely catalyzed by UV light. Cymene and ascaridole formation were added to yield total singlet oxygen formation over time, as graphed in part (c) where statistically significant results ($p \leq 0.05$) were denoted with a red star above the error bar.

photosensitizing capabilities of berberine and its analogs is key to generating an understanding of the relationship of C-ring chemical modification and photochemical properties. In this study, we synthesized two reduced analogs of berberine: dihydroberberine and tetrahydroberberine, which can both be synthesized through borohydride reduction of the pyridinium C-ring of commercially available berberine chloride and compared these analogs with berberine for singlet oxygen photosensitizing abilities using the qNMR

method we reported previously (16).

The reduction of berberine changes berberine's chromophore by decreasing conjugation, which increases the energy gap between sequential orbitals, as evidenced by a blue shift of UV-vis spectra taken of each compound and TD-DFT calculations. We found that under UV light, the singlet oxygen photosensitizing efficiency was appreciably hampered by reduction at the C-ring. This suggests that the reduction of berberine significantly impacts the electronic properties of berberine, and that the DNA binding properties of such analogs should be evaluated next to assess its properties as a DNA binding photosensitizer. However, whether this finding holds in in vivo photodynamic applications remains to be seen.

The production of singlet oxygen by the control trial can be attributed to the fact that these trials were run under UV light, which can catalyze the formation of p-cymene which was measured as a function of singlet oxygen production. Interestingly, production of cymene was much faster in the presence of berberine as a photosensitizing agent; we have not yet deduced the mechanism underlying this increase.

Despite TD-DFT analysis indicating that the reduced berberine analogs would have greater singlet oxygen efficiency than berberine, the analogs showed decreased efficacy in comparison to berberine. This may be due to differences in the irradiation spectrum that was used, as the UV lights used for irradiation did not completely overlap with the absorption spectra of the compounds.

The results from this study suggest that reduction in conjugation of the C-ring of the berberine scaffold changes the photochemical properties and UV-visible absorbance spectrum of the compound, ultimately making the reduced berberine analogs worse photosensitizers. The results from this work prompt future studies on the photodynamic biological activity of the two berberine analogs studied here, as well as other analogs of berberine with modified chromophores. Such studies are currently underway in our laboratory. Moreover, the accessibility of benchtop NMR especially poses such an experimental design to academic institutions, or in classroom settings.

MATERIALS AND METHODS

Computational Analysis

The experimental method for our computational analysis has been described in detail previously, but was enabled through geometric optimization with ORCA and Avogadro using a B3LYP functional, def-2 SVP basis set and a CPCM solvation model with the dielectric constant of deuterated acetone (16).

Photochemistry

We prepared NMR tubes with an internal standard of dimethyl terephthalate (1 eq, 8.9 mg), a solvent of d_6 -acetone (0.6 mL), alpha terpinene (1 eq, 6.25 mg), and the respective photosensitizer (10 mol%). Control NMR tubes were prepared

with the same list of conditions, but without photosensitizer. All NMR tubes were purged with oxygen. The dimethyl terephthalate was used as an internal standard to provide a basis for qNMR analysis of singlet oxygen generation, and compounds were irradiated under UV light because our compounds of interest absorb primarily UV wavelengths (22). Each reaction was performed in triplicate.

Physical Methods

Ascaridole and cymene formation were quantified through qNMR methods, wherein ¹H NMR kinetics were taken over 5 hours spread into 60 minute periods, wherein the endoperoxide group of ascaridole was characterized by a peak at 6.44 ppm (d, J = 2.28 Hz) and the cymene was characterized by a peak at 7.13 ppm (dd, J = 3.6, 2.4 Hz). Dimethyl terephthalate was used as an internal standard with peaks at 4 and 8 ppm, and NMR spectra were processed with MestreNova (23).

A more in-depth description of equipment used was described in an earlier publication (16).

Chemicals

Photosensitizers tested include berberine (MaxSun, >97%), 7,8-dihydroberberine (Synthesized), and tetrahydroberberine (Synthesized). Deuterated acetone was purchased from Martek Isotopes (>99% acetone-d₆, >99.8% deuterated), and dimethyl terephthalate (>95%) and alpha terpinene (> 95%, by GC) were purchased from AK Scientific. All compounds, other than those synthesized, were used without further purification.

Synthesis of Reduced Berberine Analogs

Treatment of berberine with sodium borohydride yielded 7,8-dihydroberberine, and treatment with excess borohydride resulted in the formation of tetrahydroberberine. The reduction of berberine to 7,8-dihydroberberine was performed with a yield of 75.4%, and the reduction of berberine to tetrahydroberberine was performed with a yield of 72%.

Statistical Analysis

Two tailed T-testing was performed to verify statistical significance; an in-depth description of our statistical methods can be found in our previous report (16).

ACKNOWLEDGMENTS

The authors declare no competing financial interests in the work expressed in this manuscript.

We would like to thank the lab technicians for ensuring our safety and helping us resolve technical issues throughout our research. Moreover, we gratefully acknowledge the Olive Children Foundation and its community of corporate sponsors and supporters for funding our research. Last but not least, we thank the Aspiring Scholars Directed Research program for providing us with lab space as well as the opportunity to conduct high-quality research.

Received: March 7, 2022

Accepted: July 19, 2022

Published: February 10, 2023

REFERENCES

1. A. Greer. "Christopher Foote's Discovery of the Role of Singlet Oxygen [¹O₂ (1Δ_g)] in Photosensitized Oxidation Reactions." *Accounts of Chemical Research*, vol. 39, no. 11, 2006, pp. 797-804, doi:10.1021/ar050191g.
2. D.A. Singleton, et al. "Mechanism of Ene Reactions of Singlet Oxygen. A Two-Step No-Intermediate Mechanism." *Journal of the American Chemical Society*, vol. 125, no. 5, 2003, pp. 1319-1328, doi: 10.1021/ja027225p.
3. A.G. Leach, et al. "Diels—Alder and Ene Reactions of Singlet Oxygen, Nitroso Compounds and Triazolinediones: Transition States and Mechanisms from Contemporary Theory." *Chemical Communications*, no. 12, 2002, pp. 1243-1255, doi: 10.1039/B111251C.
4. P.R. Ogilby. "Singlet Oxygen: There is Indeed Something New Under the Sun." *Chemical Society Reviews*, vol. 39, no. 8, 2010, pp. 3181-3209, doi: 10.1039/B926014P.
5. P. Pospíšil, Pavel, and Ankush Prasad. "Formation of Singlet Oxygen and Protection Against Its Oxidative Damage in Photosystem II Under Abiotic Stress." *Journal of Photochemistry and Photobiology B: Biology*, vol. 137, 2014, pp. 39-48, doi: 10.1016/j.jphotobiol.2014.04.025.
6. A.A. Ghogare, A. Greer. "Using Singlet Oxygen to Synthesize Natural Products and Drugs." *Chemical Reviews*, vol. 116, no. 17, 2016, pp. 9994-10034, doi: 10.1021/acs.chemrev.5b00726.
7. J.R. Kanofsky. "Singlet Oxygen Production by Biological Systems." *Chemico-Biological Interactions*, vol. 70, no. 1-2, 1989, pp. 1-28, doi: 10.1016/0009-2797(89)90059-8.
8. A.K. Balin, Vilenchik. "Oxidative Damage" *Encyclopedia of Gerontology (Second Edition)*, 2007, pp. 303-310, doi:10.1016/B0-12-370870-2/00144-X.
9. M.H. Dolmans, et al. "Photodynamic Therapy for Cancer." *Nature Reviews Cancer*, vol. 3, no. 5, 2003, pp. 380-387, doi: 10.1038/nrc1071.
10. B. Siewert, Stuppner. "The Photoactivity of Natural Products—An Overlooked Potential of Phytomedicines?." *Phytomedicine*, vol. 60, 2019, pp. 152985, doi: 10.1016/j.phymed.2019.152985.
11. K.W. Grycová, Lenka, et al. "Quaternary Protoberberine Alkaloids." *Phytochemistry*, vol. 68, no. 2, 2007, pp. 150–175, doi:10.1016/j.phytochem.2006.10.004.
12. K. Hirakawa, et al. "The Mechanism of Guanine Specific Photooxidation in the Presence of Berberine and Palmatine: Activation of Photosensitized Singlet Oxygen Generation Through DNA-Binding Interaction." *Chemical Research in Toxicology*, vol. 18, no. 10 (2005): 1545-1552.
13. K. Hirakawa, et al. "Dynamics of Singlet Oxygen Generation by DNA-Binding Photosensitizers." *The Journal of Physical Chemistry B*, vol.116, no. 9, 2012, pp. 3037-3044, doi: 10.1021/jp300142e.

14. Y. Wang, et al. "The Anti-Cancer Mechanisms of Berberine: A Review." *Cancer Management and Research*, vol. 12, 2020, pp 695–702, doi: 10.2147/CMAR.S242329.
15. F.R. Stermitz, et al. "Synergy in a Medicinal Plant: Antimicrobial Action of Berberine Potentiated by 5'-methoxyhydrnocarpin, a Multidrug Pump Inhibitor." *Proceedings of the National Academy of Sciences*, vol. 97, no. 4, 2000, pp. 1433-1437., <https://doi.org/10.1073/pnas.030540597>.
16. S. Su, Sri Indran, et al. "Comparative Singlet Oxygen Photosensitizer Efficiency of Berberine, Rose Bengal, and Methylene Blue by Time Course Nuclear Magnetic Resonance (NMR) Monitoring of a Photochemical 4+2 Cycloaddition Endoperoxide Formation." *Journal of Emerging Investigators*, vol. 4, 2021.
17. S. Sun, et al. "Strain-Specific and Photochemically-Activated Antimicrobial Activity of Berberine and Two Analogs." *Journal of Emerging Investigators*, vol. 3, 2020.
18. N.L. Andrezza, et al. "Berberine as a Photosensitizing Agent for Antitumoral Photodynamic Therapy: Insights Into Its Association to Low Density Lipoproteins." *International Journal of Pharmaceutics*, vol. 510, no. 1, 2016, pp. 240-249, doi: 10.1016/j.ijpharm.2016.06.009.
19. M.C. DeRosa, Maria C., and Robert J. Crutchley. "Photosensitized Singlet Oxygen and Its Applications." *Coordination Chemistry Reviews*, vol. 233, 2002, pp. 351-371, doi: 10.1016/S0010-8545(02)00034-6.
20. M.E. Alberto, Marta Erminia, Bruna Clara De Simone, Emilia Sicilia, Marirosa Toscano, and Nino Russo. "Rational Design of Modified Oxobacteriochlorins as Potential Photodynamic Therapy Photosensitizers." *International Journal of Molecular Sciences*, vol. 20, no. 8, 2019, pp. 2002, doi: 10.3390/ijms20082002.
21. C.A.B. Rodrigues, et al. "Synthesizing a Berberine Derivative and Evaluating Antimicrobial Activity To Reinforce with Students the Potential Significance of Small Chemical Structure Changes for Biological Systems." *Journal of Chemical Education*, vol. 95, no. 3, 2018, pp. 492-495, doi: 10.1021/acs.jchemed.7b00458.
22. H. Urano, Hikaru, Seiji Sunohara, Hirosada Ohtomo, and Norihisa Kobayashi. "Electrochemical and Spectroscopic Characteristics of Dimethyl Terephthalate." *Journal of Materials Chemistry*, vol. 14, no. 15, 2004, pp. 2366-2368, doi: 10.1039/B406093H.
23. W. Mark Robert. "MestReNova." *J. Am. Chem. Soc.* vol. 131, no. 36, 2009, pp. 13180-13180, doi: 10.1021/ja906709t.

Copyright: © 2023 Su, Le, Singh, Indran, Pal, Regan, Jain, Shah, and Njoo. All JEI articles are distributed under the attribution non-commercial, no derivative license (<http://creativecommons.org/licenses/by-nc-nd/3.0/>). This means that anyone is free to share, copy and distribute an unaltered article for non-commercial purposes provided the original author and source is credited.

Supporting Information for *“Comparative singlet oxygen production analysis of reduced berberine analogs via a 4+2 Diels Alder-like cycloaddition monitored using nuclear magnetic resonance (NMR) spectroscopy”*

1. General Information

Materials: Solvents used in all reactions and purification processes were ACS grade or higher and were used without additional purification, and were purchased from Fisher Chemical, Sigma Aldrich, Sierra Chemical Corp, Beantown Chemical, Stellar Chemical, JT Baker, or Acros Organics. Deuterated solvents were purchased from Cambridge Isotope Laboratories, Acros Organics, or Martek Isotopes, and were used without further purification. All other reagents, catalysts, and chemicals were purchased from commercial sources and used without further purification unless otherwise stated. Solvents used in analytical methods (HPLC, LCMS) were HPLC grade (22 micron filtered).

Physical methods: ^1H and $^{13}\text{C}\{^1\text{H}\}$ chemical shifts are reported in parts per million (ppm) relative to tetramethylsilane (TMS) as an internal standard. Mass spectra were obtained using a Thermo Electron LTQ-XL linear ion trap mass spectrometer equipped with a Thermo Finnigan Surveyor reverse phase high performance liquid chromatography (LC-MS) or a Thermo Scientific ISQ single quadrupole mass spectrometer equipped with a Thermo Trace 1300 gas chromatograph (GC-MS). Infrared spectra were collected on a Thermo Scientific Nicolet iS5 fourier transform infrared (FT-IR) spectrometer equipped with a Thermo iD5 attenuated total reflectance (ATR) assembly.

2. Spectroscopic Data and Experimental Procedures

Dihydroberberine

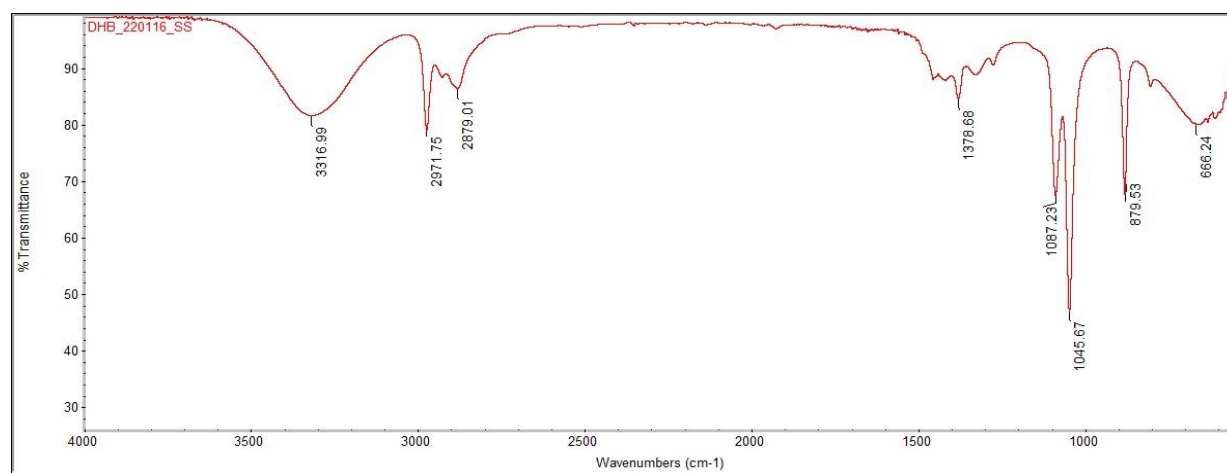
Experimental procedure: Berberine (1 eq, 1.5 g) and potassium carbonate (2.7 eq, 1.674 g) in methanol (54 mL) was added to a round bottom flask charged with a teflon stir bar. A test tube with 0.5M NaOH (9 mL) and sodium borohydride (1 eq, 168 mg) was added to the solution dropwise. Upon completion of the reaction, monitored via thin-layer chromatography (TLC), 6M HCl (4 mL) was added to the solution, and 0.1M sodium carbonate solution (100 mL) was added to precipitate 7,8-dihydroberberine out of the solution. The solution was filtered through a

Büchner funnel to yield 7,8-dihydroberberine (0.799 g, 2.36 mmol, 75.4% yield), further purified through recrystallization in ethanol.

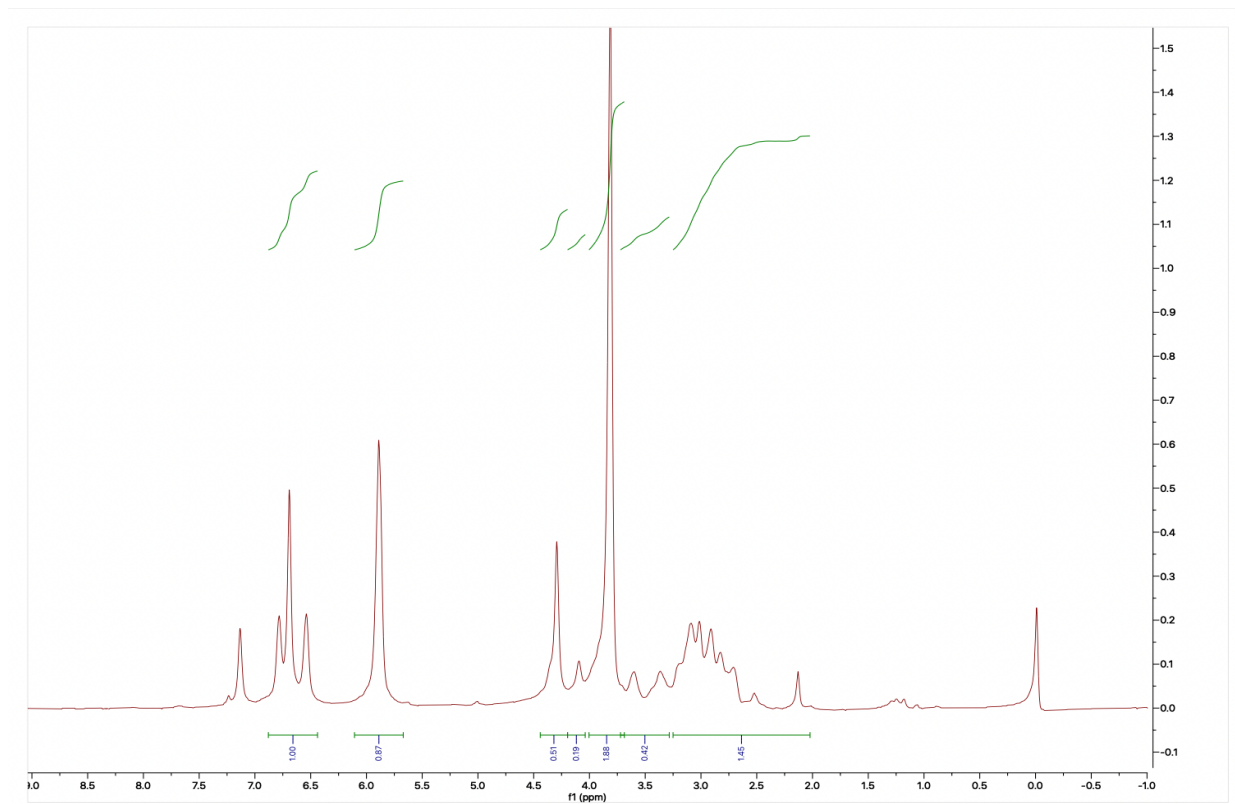
Chemicals: Methylene chloride was purchased from Stellar Chemical. Sodium borohydride was purchased from Fisher Scientific. Potassium carbonate was purchased from Cellular Science. Ethanol (ACS grade) was purchased from Bio Basic. Methanol (HPLC grade) was purchased from Duda Energy. Silica gel (230-400 mesh) was purchased from Merck, and solvents used in purification were purchased from JT Baker (ACS grade). All of the purchased solvents and reagents were used without further purification.

Dihydroberberine TLC $R_f = 0.689$ (10% Methanol / 90% Methylene Chloride),

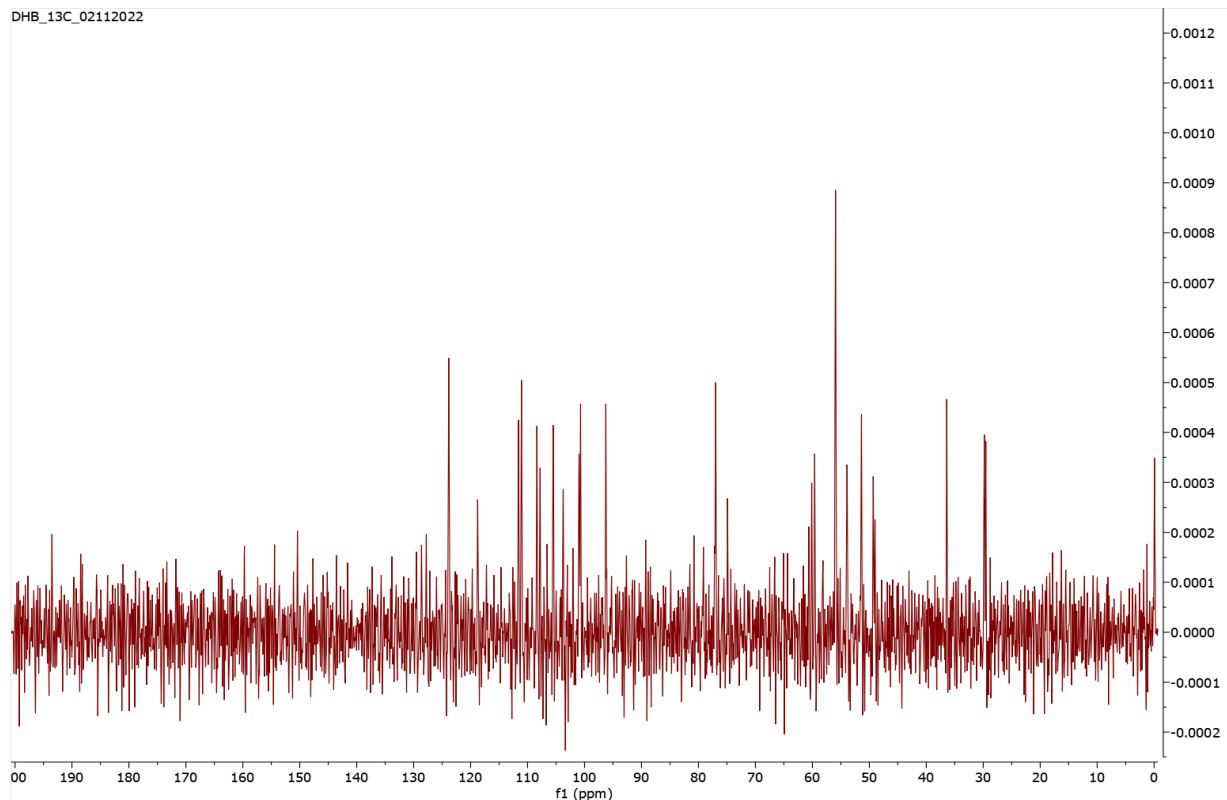
UV-vis (Acetone) $\lambda_{max} = 369$ nm



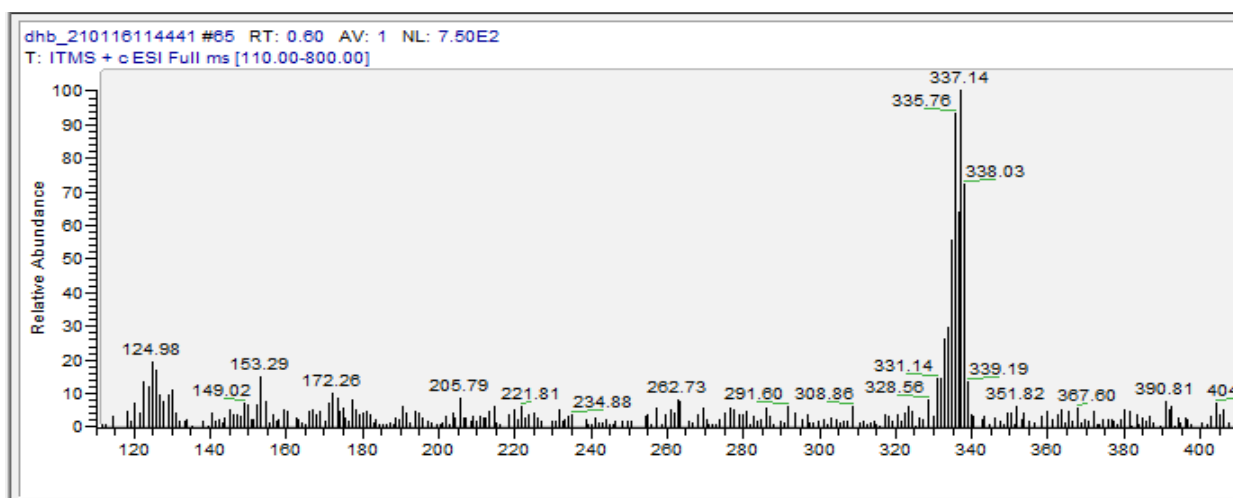
FT-IR (neat, ATR): 3316.99, 2971.75, 2879.01, 1378.68, 1087.23, 1045.67, 879.53, 666.24 cm^{-1}



¹H NMR (61 MHz, Chloroform-d) δ 6.55-6.80 (multiplet, 4H), 6.00 (s, 2H), 4.3 (s, 2H), 4.11 (s, 2H), 3.83 (s, 6H), 3.49 (dd, $J = 13.94$ Hz, 1H), 2.14-3.09 (app m, 6H).

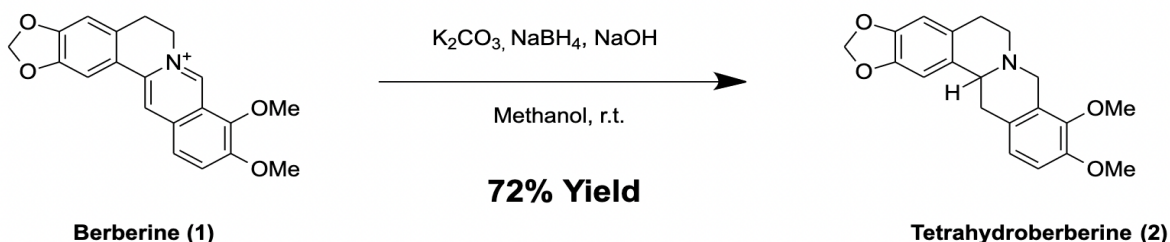


^{13}C NMR (15 MHz, Chloroform- d) δ 123.84, 111.60, 111.07, 108.38, 107.81, 105.50, 103.74, 100.96, 100.69, 96.27, 76.98, 60.10, 59.61, 55.93, 53.93, 51.38, 49.33, 36.42, 29.81, 29.54.



ESI-MS (m/z): $[\text{M}+\text{H}]^+$ calculated for $\text{C}_{20}\text{H}_{19}\text{NO}_4$: 337.131409, found: 337.14

Tetrahydroberberine

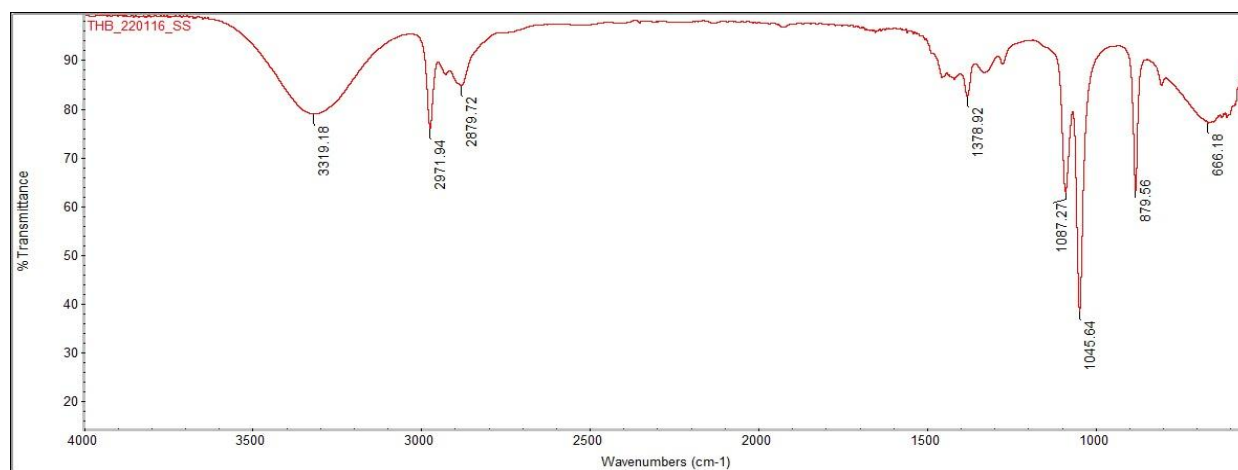


Experimental procedure: Berberine (1 eq, 1.5 g) and potassium carbonate (2.7 eq, 1.674 g) in methanol (54 mL) was added to a round bottom flask charged with a teflon stir bar. A test tube with 0.5M NaOH (9 mL) and sodium borohydride (1 eq, 168 mg) was added to the solution dropwise. The solution was stirred for 15 minutes. Upon completion of the reaction, monitored via TLC, 6M HCL (4 mL) was added to the solution, and 0.1M sodium carbonate solution (100 mL) was added to precipitate tetrahydroberberine out of the solution. The solution was filtered through a büchner funnel to yield tetrahydroberberine in 72% yield, further purified through recrystallization in ethanol.

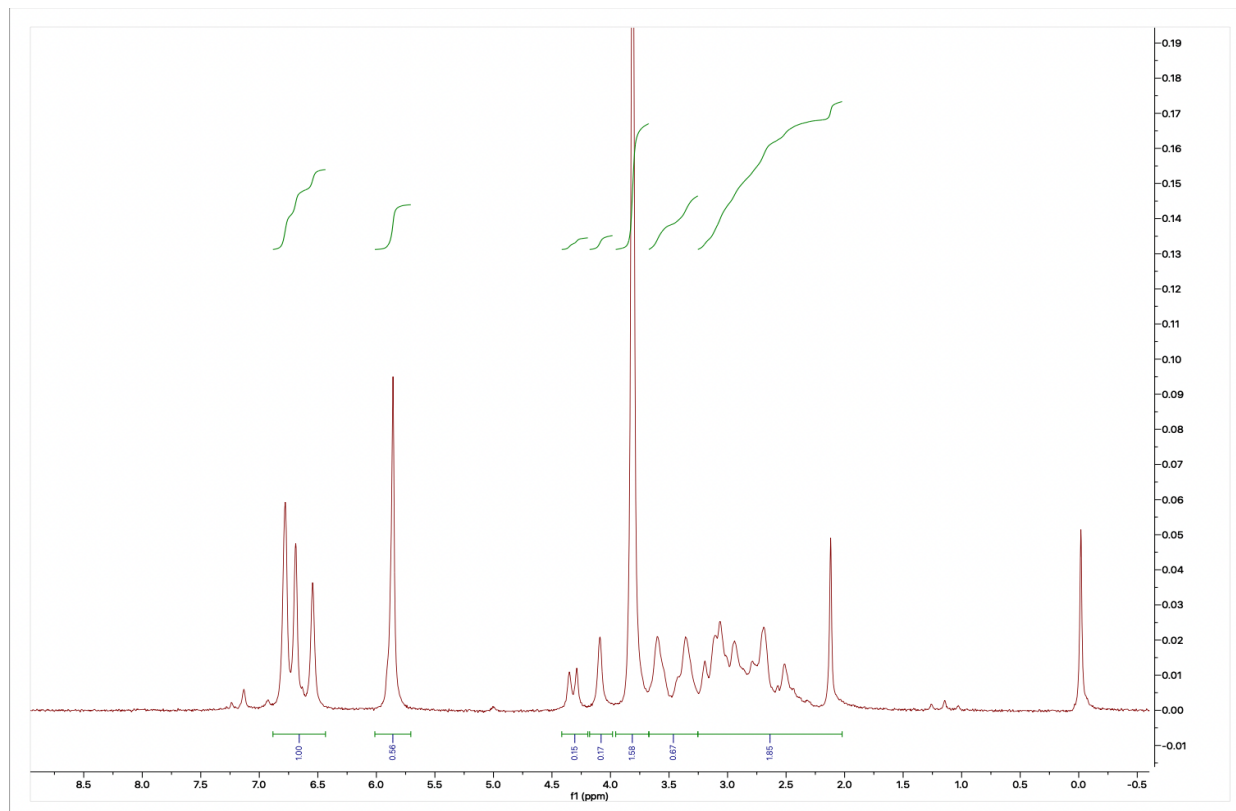
Chemicals: Berberine (MaxSun, >97%) was used. Deuterated acetone was purchased from Martek Isotopes (>99% acetone-d₆, >99.8% deuterated). Dimethyl terephthalate (>95%) and alpha terpinene (> 95%, by GC) were purchased from AK Scientific. Methylene Chloride was purchased from Stellar Chemical. Sodium Borohydride was purchased from Fisher Scientific. Potassium Carbonate was purchased from Cellular Science. Ethanol (ACS grade) was purchased from Bio Basic. Methanol (HPLC grade) was purchased from Duda Energy. Silica gel (230-400 mesh) was purchased from Merck, and solvents used in purification were purchased from JT Baker (ACS grade). All of these solvents and reagents were used without purification.

Tetrahydroberberine TLC $R_f = 0.560$ (10% Methanol / 90% Methylene Chloride)

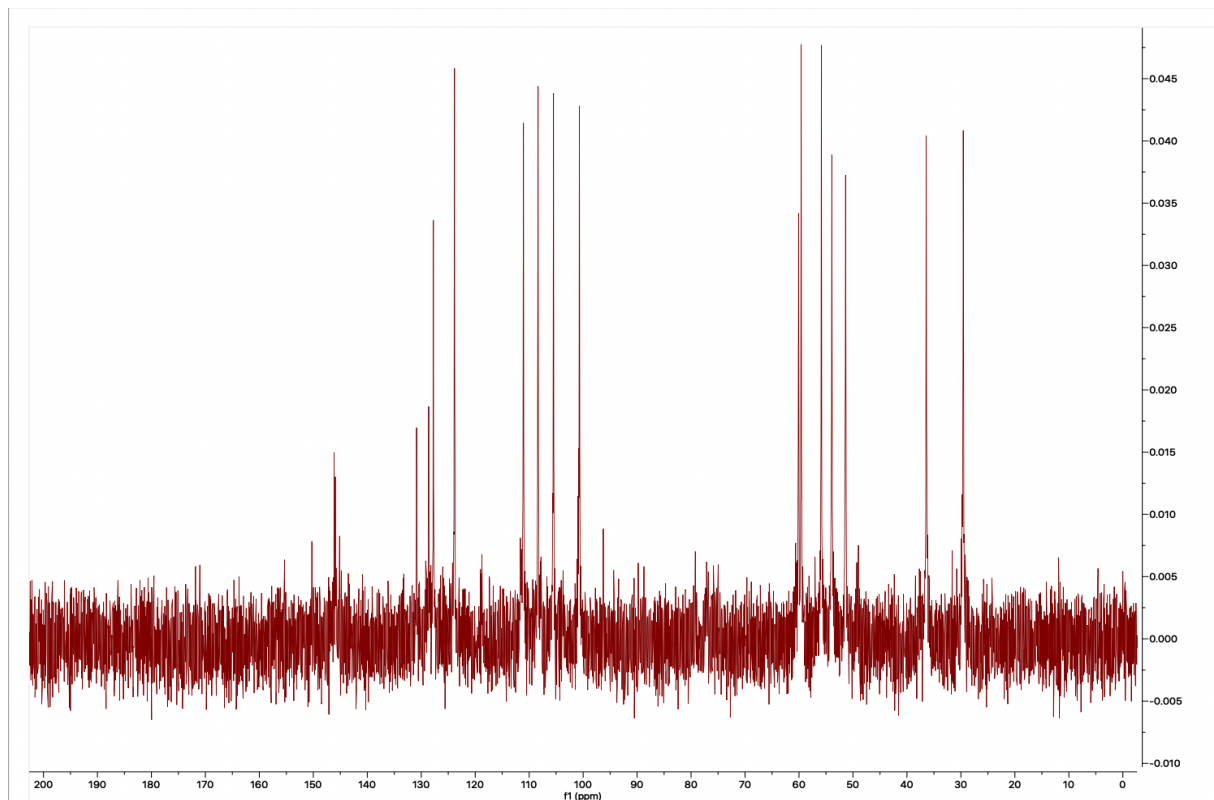
UV-vis (Acetone) $\lambda_{\text{max}} = 349$ nm



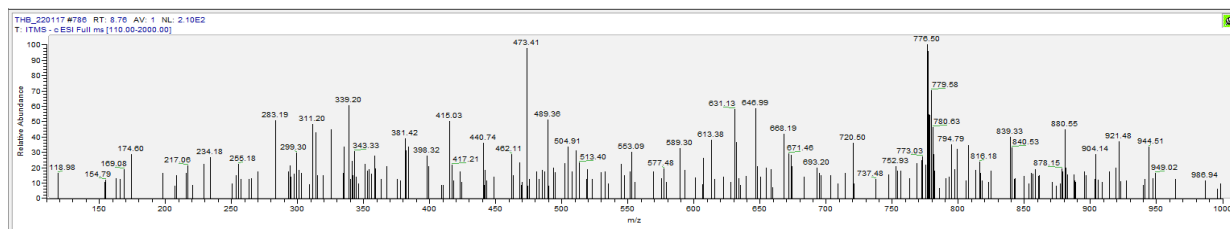
FT-IR (neat, ATR): 3319.18, 2971.94, 2879.72, 1378.92, 1087.27, 1045.64, 879.56, 666.18 cm^{-1}



^1H NMR (61 MHz, Chloroform-d) δ 6.43-6.87 (multiplet, 4H), 5.86 (s, 2H), 4.3 (dd, $J = 4.16$ Hz, 2H), 3.81 (s, 6H), 3.5 (dd, $J = 15.00$ Hz, 1H), 2.06-3.24 (app m, 6H).



^{13}C NMR (15 MHz, Chloroform- d) δ 146.15, 130.87, 128.62, 127.75, 123.83, 111.06, 108.35, 105.50, 100.70, 60.07, 59.60, 55.86, 53.92, 51.37, 36.43, 29.57.



ESI-MS (m/z): $[\text{M}+\text{H}]^+$ calc'd for $\text{C}_{20}\text{H}_{21}\text{NO}_4$: 339.147059, found: 339.20

3. *In Silico* Modeling

Compound 1

DFT-optimized structure (B3LYP def2-SVP)

* xyz 0 1 (Å)

C	-2.739000	0.701000	-0.482000
O	-1.345000	0.704000	-0.162000

C	-0.586000	0.874000	-1.287000
C	0.111000	-0.194000	-1.868000
C	0.852000	0.022000	-3.056000
C	1.522000	-1.010000	-3.719000
N	2.231000	-0.802000	-4.854000
C	2.348000	0.446000	-5.390000
C	1.687000	1.515000	-4.766000
C	0.937000	1.314000	-3.603000
C	0.275000	2.377000	-2.974000
C	-0.479000	2.158000	-1.822000
C	3.144000	0.569000	-6.629000
C	3.685000	1.798000	-7.056000
C	4.386000	1.843000	-8.246000
C	4.572000	0.730000	-9.024000
C	4.076000	-0.497000	-8.653000
C	3.374000	-0.579000	-7.439000
C	2.820000	-1.899000	-6.978000
C	2.928000	-1.965000	-5.465000
O	5.283000	0.995000	-10.150000
C	5.525000	2.410000	-9.997000
O	4.959000	2.952000	-8.782000
O	0.099000	-1.491000	-1.413000
C	0.050000	-1.663000	0.003000
H	-3.289000	0.426000	0.422000
H	-2.966000	-0.040000	-1.257000
H	-3.074000	1.696000	-0.794000
H	1.498000	-2.029000	-3.340000
H	1.737000	2.514000	-5.196000
H	0.334000	3.391000	-3.369000
H	-0.984000	2.993000	-1.341000
H	3.582000	2.717000	-6.487000
H	4.240000	-1.363000	-9.287000
H	3.379000	-2.733000	-7.417000
H	1.775000	-1.979000	-7.299000
H	3.966000	-1.918000	-5.114000
H	2.469000	-2.889000	-5.099000
H	5.089000	2.937000	-10.853000
H	6.608000	2.583000	-9.987000
H	0.488000	-2.641000	0.229000
H	-0.986000	-1.683000	0.350000
H	0.641000	-0.909000	0.535000

*

Compound 2

DFT-optimized structure (B3LYP def2-SVP)

* xyz 0 1 (Å)

C	9.83560	4.06950	-6.48693
O	8.94286	3.00142	-6.80618
C	7.70306	3.17621	-6.23290
C	6.86294	4.25213	-6.57535
O	7.34040	5.14406	-7.49947
C	6.40942	6.05756	-8.06480
C	5.60885	4.34691	-5.96755
C	5.18327	3.36796	-5.06417
C	6.00354	2.27798	-4.75631
C	7.27239	2.17551	-5.34206
C	8.14315	0.97734	-5.05791
N	7.68059	0.17705	-3.91243
C	8.54728	-0.95212	-3.56495
C	8.36099	-1.32529	-2.09583
C	6.35754	0.23929	-3.45836
C	5.91411	-0.81193	-2.48714
C	6.90223	-1.58391	-1.80790
C	6.54245	-2.55783	-0.86015
C	4.55790	-1.09059	-2.23724
C	4.23918	-2.06447	-1.31175
C	5.20250	-2.77273	-0.63805
O	4.67429	-3.67867	0.22695
C	3.26379	-3.45825	0.02075
O	2.97902	-2.43760	-0.95801
C	5.53860	1.24059	-3.83076
H	10.84868	3.65628	-6.45971
H	9.63064	4.51516	-5.50634
H	9.81104	4.83335	-7.26924
H	6.91804	6.59691	-8.86972
H	6.08639	6.79538	-7.32349
H	5.55280	5.53541	-8.50432
H	4.93248	5.16889	-6.17618
H	4.19968	3.46233	-4.60970
H	9.16338	1.31971	-4.84654
H	8.16683	0.34133	-5.95144
H	9.60047	-0.69939	-3.73551
H	8.30515	-1.80416	-4.21314
H	8.70727	-0.51330	-1.44484
H	8.96181	-2.21500	-1.87493
H	7.28826	-3.13356	-0.32355
H	3.75577	-0.57546	-2.75125

H	2.81162	-3.16465	0.97515
H	2.80684	-4.39808	-0.31001
H	4.52936	1.34326	-3.45346

*

Compound 3
DFT-optimized structure (B3LYP def2-SVP)

* xyz 0 1 (Å)

C	-6.87141	0.45209	-0.28235
C	-5.42192	-0.11182	-0.32085
N	-4.45375	0.95382	-0.70387
C	-4.73924	1.48063	-2.04734
C	-4.77058	0.42334	-3.16329
C	-5.10702	-0.50943	1.15722
C	-3.66724	-0.86469	1.40857
C	-3.31534	-1.66286	2.50577
C	-1.97648	-1.94914	2.76699
C	-0.97883	-1.43277	1.94303
O	0.30765	-1.76106	2.28355
C	1.13445	-0.60917	2.45152
C	-1.32974	-0.67380	0.81784
O	-0.37880	-0.22315	-0.06627
C	0.05435	-1.29718	-0.90595
C	-2.67389	-0.33777	0.57162
C	-3.04134	0.50467	-0.62814
C	-5.43243	-1.25995	-1.34709
C	-5.17051	-0.96790	-2.71977
C	-5.21553	-1.98532	-3.69042
C	-5.75048	-2.58231	-0.98268
C	-5.77954	-3.55136	-1.96435
C	-5.52031	-3.26225	-3.27963
O	-5.59863	-4.35843	-4.07983
C	-5.92915	-5.37547	-3.11164
O	-6.06122	-4.86788	-1.76795
H	-6.92690	1.36560	0.32178
H	-7.56214	-0.27585	0.16206
H	-7.26858	0.68365	-1.27712
H	-4.01312	2.26178	-2.30921
H	-5.69772	2.01317	-2.03066
H	-3.76817	0.35417	-3.60547
H	-5.45407	0.76020	-3.95212
H	-5.75653	-1.32574	1.49334
H	-5.33087	0.34283	1.81613

H	-4.08252	-2.05859	3.16724
H	-1.70876	-2.56263	3.62267
H	1.91675	-0.86625	3.17242
H	0.58415	0.25165	2.84903
H	1.62616	-0.35074	1.50949
H	0.68057	-0.86941	-1.69460
H	-0.79346	-1.80059	-1.38476
H	0.66070	-2.01929	-0.35038
H	-2.75899	-0.07536	-1.51453
H	-2.41708	1.40720	-0.61411
H	-5.00529	-1.78176	-4.73499
H	-5.97605	-2.86927	0.03693
H	-5.14229	-6.13869	-3.12236
H	-6.87619	-5.84323	-3.40418

*